Framework Structure, Phase Transition, and Transport Properties in $M^{II}Zr_4(PO_4)_6$ Compounds (M^{II}=Mg, Ca, Sr, Ba, Mn, Co, Ni, Zn, Cd, and Pb)

Katsuhiro NOMURA,* Shoichiro IKEDA, Kaname ITO, and Hisahiko EINAGA
Department of Applied Chemistry, Faculty of Engineering, Nagoya Institute of Technology, Gokiso-cho, Showa-ku, Nagoya 466
(Received June 19, 1992)

The crystal structure, phase transition, electrical conduction behavior of various kinds of $M^{II}Zr_4(PO_4)_6$ ($M^{II}ZP$) compounds (M^{II}=Mg, Ca, Sr, Ba, Mn, Co, Ni, Zn, Cd, and Pb) have been investigated. The Mg, Co, Ni, and Zn compounds are of the β-$Fe_2(SO_4)_3$-type structure and show an order–disorder transition between 600 and 720 °C; the Ca, Sr, Ba, Cd, and Pb compounds, however, are of the NASICON-type structure and do not show any phase transition between r.t. and 1000 °C. The Mn compound sintered at 900 °C shows the former characteristics (the phase transition temperature is around 560 °C), and that sintered above 900 °C the latter. The ZnZP and MnZP show the highest conductivity, ca. 2×10^{-3} and ca. 8×10^{-4} S cm^{-1} at 800 °C, in the β-$Fe_2(SO_4)_3$- and the NASICON-type structure, respectively. The ionic size of the mobile cation is the predominant factor regarding ionic conduction in the zirconium phosphate framework.

Since 1976[1,2] numerous studies have been carried out on NASICON (Na super ionic conductor, $Na_{1+x}Zr_2P_{3-x}Si_xO_{24}$ ($0\leqq x\leqq3$)) and its analogous compounds in order to prepare solid electrolytes having high conductivity and stability. They equally contain monovalent cations as a charge carrier.

In our previous studies, we reported new divalent cationic conductors of $MgZr_4(PO_4)_6$[3] and $ZnZr_4(PO_4)_6$;[4] they belong to a β-$Fe_2(SO_4)_3$-type structure.[5,6] This three-dimensional skeletal structure comprises PO_4 tetrahedra sharing corners with ZrO_6 octahedra. The $Zr_2P_3O_{18}$ (lantern) units in the β-$Fe_2(SO_4)_3$-type structure are similar to those found in the NASICON-type structure, but their arrangements are different. We have also reported that the ionic conductivity in the β-$Fe_2(SO_4)_3$-type structure is not determined by only the ionic radius of the guest cation.[5]

In the present work we performed a systematic investigation on the framework structure, the phase transition, and the electrical conduction behavior of various kinds of $M^{II}Zr_4(PO_4)_6$ ($M^{II}ZP$; M^{II}=Mg, Ca, Sr, Ba, Mn, Co, Ni, Zn, Cd, and Pb) compounds. Divalent cations having different ionic sizes and polarizabilities were selected in order to understand more clearly the mutual interaction between a mobile cation and the zirconium phosphate framework.

Experimental

Sample Preparation. Samples were prepared using a sol–gel method based on the same procedure as mentioned in a preceding paper.[5] The starting materials were of reagent-grade $M^{II}(NO_3)_2\cdot nH_2O$ (M^{II}=Mg, Ca, Sr, Ba, Mn, Co, Ni, Zn, Cd, and Pb), $ZrOCl_2\cdot8H_2O$ or $ZrO(NO_3)_2\cdot2H_2O$ (for PbZP), and $NH_4H_2PO_4$. The powder prepared by the sol–gel method was pressed uniaxially under 9.8 MPa and then isostatically under 490 MPa into a tablet. The tablet was covered with powder of the same composition and then sintered in an alumina boat at 900, 1000, 1100, 1200, 1300, or 1400 °C for 24 h in air.

Characterization. The chemical composition of the sample was determined with an Inductively-Coupled-Plasma (ICP) Emission Spectrometer (Model SPS 7000A of Seiko Instruments, Inc.).

Crystallographic characterization was achieved through a powder X-ray diffraction (XRD) analysis with a diffractometer (Model RAD-2A of Rigaku Denki Co., Ltd.) using Cu $K\alpha$ radiation. The crystal system and lattice parameters were determined using a least-squares computer program.

Complex impedance measurements were made on a frequency-response analyzer (Model Solartron 1255 of Schlumberger Technologies) over the frequency range 0.2 Hz to 2 MHz at temperatures between 500 and 900 °C. The sample surface was polished to 1500 grit; gold was then evaporated in vacuum so that good contact between the Pt foil electrodes and the solid electrolyte could be obtained. Each run was made either in air or in flowing Ar (100 cm^3 min^{-1}).

The ionic transport number was measured using a modified Tubandt method with Pt electrodes in air.[3,4] In order to confirm that the conduction of $M^{II}ZP$ was caused by ionic migration, the XRD for the sample surface attached with a Pt electrode and the line profile analysis for the sample cross section by Electron Prove Micro Analysis (EPMA) were also carried out for the sample both before and after electrolysis. The electronic conductivity was determined by a dc-polarization method using Pt electrodes in flowing Ar (100 cm^3 min^{-1}).[7,8]

Differential thermal analysis (DTA) was carried out using an apparatus (Model 8121BH of Rigaku Denki Co., Ltd.) between r.t. and 1000 °C at a heating or cooling rate of 5 K min^{-1} in air.

Sample densities were measured with the Archimedes method using 1-butanol as a solvent.

Results

Chemical Composition. The chemical composition of all $M^{II}ZP$ samples agreed well with that expected

Table 1. Crystal System and Lattice Parameters of $M^{II}Zr_4(PO_4)_6$ (M^{II}=Ni, Mg, Zn, Co, Mn, Cd, Ca, Sr, Pb, and Ba) Sintered at 1100 °C

Substance	Crystal system	Lattice parameters				Cell volume	Ionic[a] radius of
		a/Å	b/Å	c/Å	β/°	V/Å^3	M^{2+}/Å
$NiZr_4(PO_4)_6$	Monoclinic	8.863	8.888	12.408	90.64	977.4	0.83
$MgZr_4(PO_4)_6$[b]	Monoclinic	8.851	8.895	12.425	90.60	978.2	0.86
$ZnZr_4(PO_4)_6$	Monoclinic	8.836	8.930	12.476	90.81	984.3	0.88
$CoZr_4(PO_4)_6$[b]	Monoclinic	8.853	8.924	12.434	90.35	982.3	0.89
$MnZr_4(PO_4)_6$[c]	Monoclinic	8.846	8.975	12.501	90.05	992.5	0.97
$MnZr_4(PO_4)_6$	Trigonal	8.843	—	21.824	—	1478	0.97
$CdZr_4(PO_4)_6$	Trigonal	8.824	—	22.292	—	1503	1.09
$CaZr_4(PO_4)_6$	Trigonal	8.778	—	22.667	—	1512	1.14
$SrZr_4(PO_4)_6$	Trigonal	8.704	—	23.443	—	1538	1.32
$PbZr_4(PO_4)_6$	Trigonal	8.682	—	23.456	—	1531	1.33
$BaZr_4(PO_4)_6$	Trigonal	8.651	—	23.977	—	1554	1.49

a) Ref. 10. b) Ref. 5. c) Sample sintered at 900 °C.

within the experimental errors.

Crystal Structure. The crystal systems, lattice parameters, and cell volumes of $M^{II}ZP$ sintered at 1100 °C are listed in Table 1 together with the ionic radii[9] of guest cations. In these compounds no peaks of the second phases of ZrP_2O_7, $Zr_2O(PO_4)_2$, ZrO_2, etc., were observed with XRD. The crystal structure of $M^{II}ZP$ did not change with the sintering temperature, except for MnZP. The Ni, Mg, Zn, and Co compounds showed almost the same X-ray diffraction patterns as did that of $LiZr_2(PO_4)_3$ sintered at 900 °C.[10] These compounds could be indexed based on a monoclinic symmetry (β-$Fe_2(SO_4)_3$-type structure). On the other hand, the Cd, Ca, Sr, Pb, and Ba compounds had a trigonal symmetry (NASICON-type structure). The Mn compound sintered at 900 °C was monoclinic (β-$Fe_2(SO_4)_3$-type structure), whereas that sintered above 900 °C was trigonal (NASICON-type structure). It is evident from these results that $M^{II}ZP$ retains the NASICON-type structure when the ionic radius of the guest cation is larger than ca. 0.97 Å.

In the monoclinic system lattice parameters b and c become larger and β smaller with an increase in the size of the guest cation, except for ZnZP. On the other hand, in the trigonal system, parameter c becomes larger and parameter a slightly smaller with an increase in the size of the guest cation. The cell volume of $M^{II}ZP$ becomes larger with increasing size of the guest cations for both systems, except for ZnZP.

Electrical Conductivity. The $M^{II}ZP$ specimens generally show two semi-circles in their complex impedance plots. Of these semi-circles, the high-frequency one, which almost passes through the origin, was assigned to the impedance of the solid electrolyte (bulk plus grain boundary), and the low-frequency one to that of electrode–electrolyte interface.

Figure 1 shows conductivity data plots (in air) of $M^{II}ZP$ specimens sintered at their optimum temperatures. The conductivity data of the Mn compound sintered at 900 °C (the β-$Fe_2(SO_4)_3$-type structure, the relative density being ca. 90%) are also plotted in Fig. 1. (The conductivity data were uncorrected regarding sample porosity.) The conductivity data measured in flowing Ar were almost the same as those in air. Those

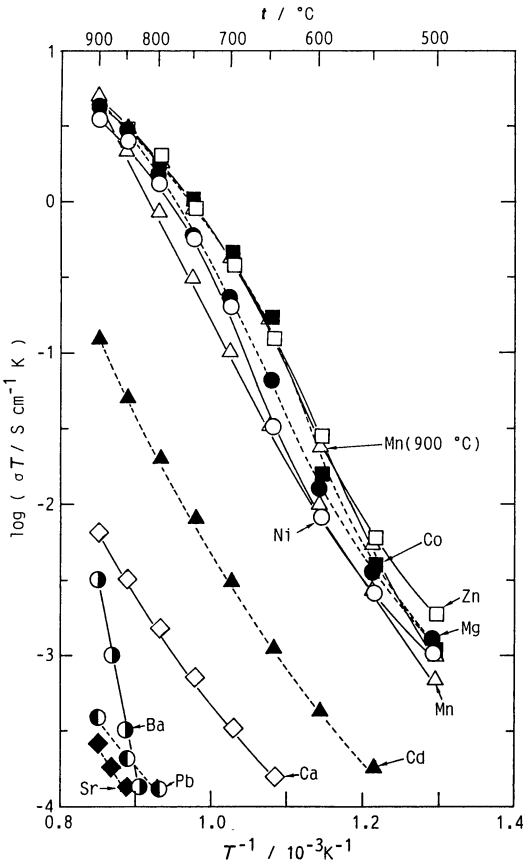

Fig. 1. Arrhenius plots of the electrical conductivities of $M^{II}Zr_4(PO_4)_6$ (M^{II}=Ni(○), Mg(●), Zn(□), Co(■), Mn(△), Cd(▲), Ca(◇), Sr(◆), Pb(◐), and Ba(◑)). Ni, Mg, Zn, Co, and Cd compounds (sintered at 1100 °C), Ca, Sr, and Ba compounds (sintered at 1400 °C), and Mn compounds (sintered at 900 or 1100 °C).

Table 2. Conductivities and Apparent Activation Energies of $M^{II}Zr_4(PO_4)_6$

Substance	t/ °C	σ/S cm^{-1}	Temperature range/ °C	E_a/kJ mol^{-1}
$NiZr_4(PO_4)_6$	500	1.3×10^{-6}	500—550	123
	800	1.2×10^{-3}	800—850	96
$MgZr_4(PO_4)_6$[a]	500	1.6×10^{-6}	500—550	110
	800	1.4×10^{-3}	800—850	96
$ZnZr_4(PO_4)_6$[a]	500	2.3×10^{-6}	500—550	120
	800	1.9×10^{-3}	800—850	82
$CoZr_4(PO_4)_6$	500	1.3×10^{-6}	500—550	134
	800	1.7×10^{-3}	800—850	82
$MnZr_4(PO_4)_6$	500	8.5×10^{-7}	500—550	144
	800	8.3×10^{-4}	800—850	187
$CdZr_4(PO_4)_6$	800	1.9×10^{-5}	800—850	183
$CaZr_4(PO_4)_6$	800	1.4×10^{-6}	800—850	146
$SrZr_4(PO_4)_6$	850	1.2×10^{-7}	850—900	141
$PbZr_4(PO_4)_6$	850	1.9×10^{-7}	850—900	136
$BaZr_4(PO_4)_6$	850	2.8×10^{-7}	850—900	504

a) Ref. 5.

specimens of the Ni, Mg, Zn, Co, Mn, Cd, and Pb compounds sintered at 1100 °C showed the highest conductivities with their relative densities above 95% of theoretical values. On the other hand, those specimens of the Ca, Sr, and Ba compounds gave the highest conductivities after sintering at 1400 °C with relative densities of ca. 85%. It is evident from Fig. 1 that the conductivity changes with M^{II} over a wide range, e.g., (ca. four orders) from ca. 10^{-3} S cm^{-1} for ZnZP to ca. 10^{-7} S cm^{-1} for SrZP at 900 °C according to the cationic size of M^{2+}; it also shows that the Ni, Mg, Zn, Co, and Mn compounds having the β-$Fe_2(SO_4)_3$-type structure, with the size of the guest cation being smaller than 0.89 Å, show a change in an activation energy in a temperature range of 560 to 720 °C caused by an order–disorder phase transition.[11] It is further seen that the Mn, Cd, Ca, Sr, Pb, and Ba compounds having the NASICON-type structure show almost a linear (Arrhenius-type) behavior, and that the apparent activation energy for the conduction also changes with the ionic radius of M^{2+} (cf. Table 2). The MgZP and ZnZP are the highest among the divalent $M^{II}ZP$ cationic conductors; they have lower activation energies than the others at ca. 850 °C.

Charge Carriers. Tubandt Method: The observed and calculated weight changes by the Tubandt method are listed in Table 3. The observed weight change of each tablet agrees with the calculated one within the experimental errors. The observed weight changes for the Ni, Co, Mn, and Ca compounds also correspond to the calculated ones when the formation of ZrO_2 is assumed.

An XRD analysis showed that the diffraction pattern of the anodically polarized surface of the specimen was almost the same both before and after electrolysis. However, the cathodically polarized surface showed additional peaks resulting from the oxides of divalent cations: The following colored precipitates were noticed by visual inspection: NiZP (dark green), CoZP

Table 3. Weight Changes of Specimen Tablets of $M^{II}Zr_4(PO_4)_6$ after Electrolysis with Modified Tubandt's Method

Substance	Q/C[a]	Tablet[b]	Weight change of tablet/mg			
			Obsd value	Calcd value for		
				M^{2+}	Zr^{4+}	O^{2-}
$NiZr_4(PO_4)_6$	10	C	+3.3	+3.87	+3.19	0.00
		M	−1.1	0.00	0.00	0.00
		A	−1.7	−3.87	−3.19	0.00
$MgZr_4(PO_4)_6$[c]	20	C	+3.8	+4.18	+6.38	0.00
		M	+0.3	0.00	0.00	0.00
		A	−4.4	−4.18	−6.38	0.00
$ZnZr_4(PO_4)_6$[d]	20	C	+9.2	+8.43	+6.38	0.00
		M	−2.2	0.00	0.00	0.00
		A	−5.9	−8.43	−6.38	0.00
$CoZr_4(PO_4)_6$	10	C	+2.8	+3.88	+3.19	0.00
		M	−1.2	0.00	0.00	0.00
		A	−2.0	−3.88	−3.19	0.00
$MnZr_4(PO_4)_6$	7	C	+2.6	+1.91	+2.23	0.00
		M	0.0	0.00	0.00	0.00
		A	−2.0	−1.91	−2.23	0.00
$CdZr_4(PO_4)_6$	2	C	+1.5	+1.33	+0.64	0.00
		M	−0.2	0.00	0.00	0.00
		A	−1.4	−1.33	−0.64	0.00
$CaZr_4(PO_4)_6$	5	C	+1.4	+1.45	+1.60	0.00
		M	−1.0	0.00	0.00	0.00
		A	−0.6	−1.45	−1.60	0.00
$SrZr_4(PO_4)_6$	3	C	+1.8	+1.61	+0.96	0.00
		M	−0.5	0.00	0.00	0.00
		A	−1.0	−1.61	−0.96	0.00
$PbZr_4(PO_4)_6$	3	C	+3.1	+3.47	+0.96	0.00
		M	−1.2	0.00	0.00	0.00
		A	−1.8	−3.47	−0.96	0.00
$BaZr_4(PO_4)_6$	3	C	+2.2	+2.38	+0.96	0.00
		M	−0.4	0.00	0.00	0.00
		A	−1.9	−2.38	−0.96	0.00

a) Q: Quantity of electricity for electrolysis. b) C: Cathodic side, M: Middle side, A: Anodic side. c) Ref. 3. d) Ref. 4.

Table 4. Electronic Transport Numbers of $M^{II}Zr_4(PO_4)_6$ Compounds

Substance	σ_t[a)]/S cm^{-1}	σ_e[b)]/S cm^{-1}	t_e[c)]	t/ °C	Color
$NiZr_4(PO_4)_6$	1.86×10^{-3}	2.74×10^{-6}	0.0015	800	Brown
$MgZr_4(PO_4)_6$	3.42×10^{-3}	6.71×10^{-6}	0.0019	800	White
$ZnZr_4(PO_4)_6$	1.16×10^{-3}	1.71×10^{-6}	0.0015	800	White
$CoZr_4(PO_4)_6$	7.54×10^{-4}	2.94×10^{-6}	0.0039	800	Dark blue
$MnZr_4(PO_4)_6$	1.31×10^{-3}	4.89×10^{-6}	0.0037	800	Light pinc
$CdZr_4(PO_4)_6$	1.17×10^{-5}	1.31×10^{-7}	0.011	800	White
$CaZr_4(PO_4)_6$	6.77×10^{-6}	9.00×10^{-8}	0.013	900	White
$SrZr_4(PO_4)_6$	2.34×10^{-7}	1.22×10^{-8}	0.052	900	White
$PbZr_4(PO_4)_6$	4.48×10^{-7}	6.59×10^{-8}	0.147	900	White
$BaZr_4(PO_4)_6$	8.93×10^{-7}	9.77×10^{-8}	0.109	900	White

a) Total electrical conductivity. b) Electronic conductivity. c) Electronic transport number ($t_e=\sigma_e/\sigma_t$).

(brown), MnZP (black), CdZP (brown), and PbZP (yellow).

A line-profile analysis of the constituent elements by EPMA supported the results by XRD: Although M, Zr, and P were homogeneously present in the specimen from the anodic to cathodic side before the electrolysis, the accumulation of M with concomitant decreases of P and Zr was observed at the cathodic side after electrolysis.

Hence, it is concluded that M^{2+} is the main charge carrier in the $M^{II}ZP$ (M^{II}=Ni, Mg, Zn, Co, Mn, Cd, Ca, Sr, Pb, and Ba) compounds.

Dc Polarization Method: The electronic transport numbers (t_e) of $M^{II}ZP$ at 800 or 900 °C in Ar are listed in Table 4, together with the total electrical (σ_t) and electronic (σ_e) conductivities. The electronic transport number becomes larger with an increase in the ionic size of M^{2+}. The Ni, Mg, Zn, Co, and Mn compounds may be taken as ionic conductors, because their electronic transport numbers are less than 0.01. On the other hand, the Cd, Ca, Sr, Pb, and Ba compounds are almost ionic conductors.

The Tubandt and dc polarization methods allow us to classify the Ni, Mg, Co, Zn, and Mn compounds as pure ionic conductors, whereas the Cd, Ca, Sr, Pb, and Ba compounds are classified mainly as ionic conductive solids.

Phase Transition. The structural characteristics of the framework of $M^{II}ZP$ at high temperature, as studied by DTA, showed that the Ni, Mg, Zn, Co, and Mn compounds, which belong to the β-$Fe_2(SO_4)_3$-type, have a small, but reversible, peak: i.e. an exothermic peak produced upon heating and an endothermic peak produced upon cooling. The transition temperature estimated from the DTA peak is as follows: 710—720 °C (NiZP), 670—680 °C (MgZP), 670—680 °C (ZnZP), 600—620 °C (CoZP), and 560—570 °C (MnZP sintered at 900 °C). The peak temperature was found to decrease with increasing the ionic radius of the guest cation. These small, but reversible, peaks of the β-$Fe_2(SO_4)_3$-type $M^{II}ZP$ are expected to arise from an order-disorder transition. On the contrary, no phase transition was noticed for the NASICON-type $M^{II}ZP$.

Discussion

Crystal Structure. $M^{II}ZP$ compounds crystallize into the β-$Fe_2(SO_4)_3$-type (M^{II}: Ni, Mg, Zn, and Co) or NASICON-type (M^{II}: Cd, Ca, Sr, Pb, and Ba) structure according to the guest cation, except for MnZP, which crystallizes into the former when sintered at 900 °C, and the latter when sintered above 900 °C. These structural characteristics can be understood in terms of the correlation between the size of guest cation and the site in which it is accommodated.

In the zirconium phosphate framework with the NASICON-type structure, there are two sites (M_1 and M_2[1)]) which the guest cations can occupy. The M_1 site is situated in the octahedra formed by the triangular faces of two ZrO_6 octahedra in the endless columns of

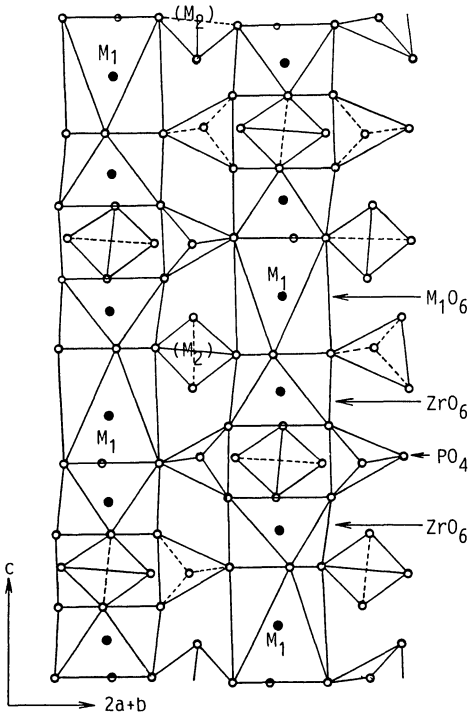

Fig. 2. NASICON-type structure (M_1: M_1 site, and M_2: M_2 site).

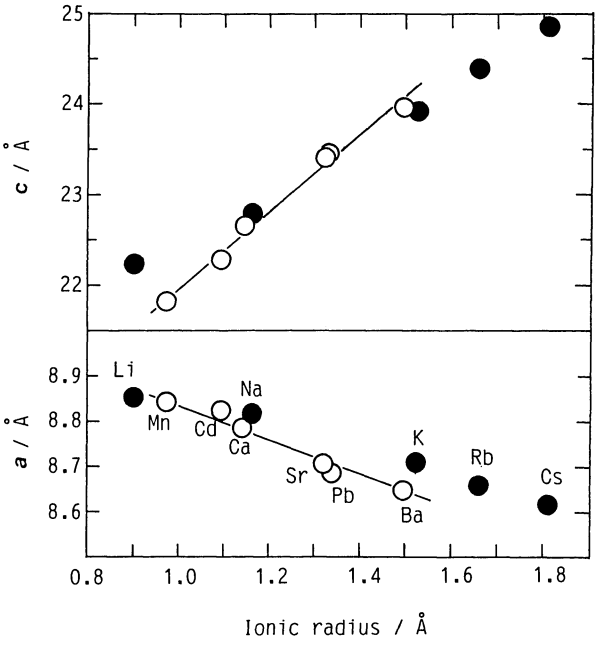

Fig. 3. Lattice parameters as a function of the ionic radius of the guest cation for $M^{I}Zr_2(PO_4)_3$[a] (M^{I}=Li, Na, K, Rb, and Cs) and $M^{II}Zr_4(PO_4)_6$ (M^{II}=Mn, Cd, Ca, Sr, Pb, and Ba) compounds with NASICON-type structure.
a) Refs. 13, 14, and 15.

$O_3ZrO_3M_1O_3ZrO_3$ (*c*-axis direction), while the M_2 site is between the endless columns (cf. Fig. 2). Consequently, if the guest cation occupies the M_1 site, the *c*-axis should change with the cationic size.[12] Figure 3 shows the relationship between the lattice parameters and the ionic radius of the $M^{II}ZP$ compounds with the NASICON-type structure. In this figure are also plotted those of $M^{I}Zr_2(PO_4)_3$ compounds (M^{I}: Li, Na, K, Rb, and Cs), where the guest cation occupies the M_1 site,[13–15] for a comparison. The *c*-axis markedly increases, while the *a*-axis slightly decreases with an increase in the cationic size for both $M^{I}Zr_2(PO_4)_3$ and $M^{II}Zr_4(PO_4)_6$ compounds. Incidentally, the divalent cation compounds show slightly smaller lattice parameters, due to the stronger interaction between the guest cation and the framework. Thus, the divalent cations are expected to occupy the M_1 site in the zirconium phosphate framework just as the monovalent cations, although the population of the former is half that of the latter. The larger guest cation in the host framework is expected to enlarge the M_1 site by rotating the PO_4 tetrahedra about a two-fold rotation axis and the ZrO_6 octahedra about a three-fold axis.[15] On the other hand, the smaller guest cation accompanies a space between the cation and the framework oxygen, which brings about a structural transformation of the NASICON- into the β-$Fe_2(SO_4)_3$-type. The guest cation is expected to occupy a four-coordination site[9] in the β-$Fe_2(SO_4)_3$-type structure; the exact position of M^{2+} ions will be reported elsewhere.[16] The results given in Table 1 demonstrate that the Mn^{2+} ion of 0.97 Å is of the critical size in the zirconium phosphate framework for its structural morphology.

The structural change with sintering temperature, found in MnZP, has also been reported for $LiZr_2(PO_4)_3$ (LiZP).[9] The structural change of LiZP is, however, more gradual than that of MnZP; LiZP sintered at 900 and 1200 °C is of the β-$Fe_2(SO_4)_3$- and NASICON-type, respectively; that sintered between 900 and 1200 °C is a mixture of these two types. Further, the ionic radius of Li^+ (0.90 Å) is slightly smaller than that of Mn^{2+} ion. Hence, this difference can be ascribed to a difference in the charge density of the guest cation; a stronger interaction between the Mn^{2+} ion and the zirconium phosphate framework will cause a steep structural change from the NASICON- to the β-$Fe_2(SO_4)_3$-type structure.

Conductivity. The data plotted in Fig. 1 correspond to the total (bulk plus grain boundary) conductivities of $M^{II}ZP$. A good correlation between the conduction behavior and the powder XRD analysis and DTA data indicates that the conduction behavior of $M^{II}ZP$ should be considered while taking the structural characteristics of zirconium phosphate framework into consideration.

(i) NASICON-Type Structure: According to Hong,[1] the M^+ ion channel in NASICON ($Na_{1+x}Zr_2P_{3-x}Si_xO_{12}$, $0 \leqq x \leqq 3$) lies between the M_1 and M_2 sites (cf. Fig. 2). Kohler et al.[17,18] examined the diffusion pathway in this structure and established that the pathway from M_1 to M_2 has a zig-zag shape and that the real bottle-neck of the conduction pathway is different from, but is near to, a geometrical bottle-neck comprising the triangle formed by the oxygen of M_1O_6. In the present study the divalent cations, the ionic sizes of which correspond to those of the Li^+ to K^+ ions, have proved to occupy the M_1 site in $M^{II}ZP$ with the NASICON-type structure. On the basis of the information given above we can expect that a $M^{II}ZP$ compounds with the NASICON-type structure have a conduction pathway of the M_1-M_2-M_1 channel.

Each $M^{II}ZP$ compound with the NASICON-type structure has a large apparent activation energy for cationic conduction with no phase transition. This large activation energy may be required to migrate the M^{2+} ion from the more energetically stable M_1 to the less stable M_2 site while expanding the framework oxygens.

(ii) β-$Fe_2(SO_4)_3$-Type Structure: A few NASICON-like compounds with the β-$Fe_2(SO_4)_3$-type structure have so far been reported: $Li_3Fe_2(PO_4)_3$,[19,20] $Li_3Sc_2(PO_4)_3$,[20,21] etc. These compounds have the same framework structure as do those of the $M^{II}ZP$ compounds; the position of guest cations in the former, however, is supposed to be different from that of the latter. Since the distribution of the M^{2+} ion in the β-$Fe_2(SO_4)_3$-type framework has not been investigated, the ionic conduction behavior is not presently well-understood. However, this structure can be regarded as being another promising candidate with three-

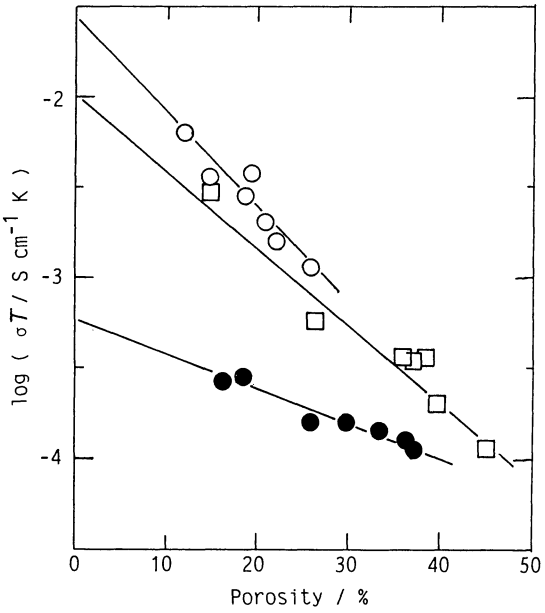

Fig. 4. Conductivity as a function of the porosity for $M^{II}Zr_4(PO_4)_6$ (M^{II}=Ca(○), Sr(●), and Ba(□)).

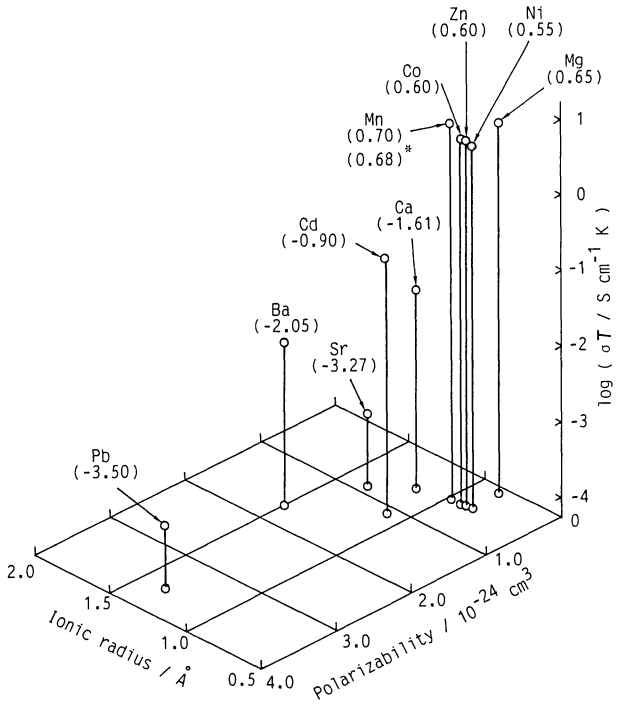

Fig. 5. Conductivity[a–c] as functions of the ionic radius[d] and the electronic polarizability[e] of a mobile cation for $M^{II}Zr_4(PO_4)_6$ compounds (M^{II}=Ni, Mg, Zn, Co, Mn, Cd, Ca, Sr, Ba, and Pb).
a) The numbers in parentheses represent conductivities.
* represents Mn compound sintered at 900 °C.
b) All of the conductivity data were corrected by multiplying by the ionic transport number.
c) The conductivity data of Ca, Sr, and Ba compounds were corrected regarding their porosity (cf. Fig. 4).
d) Ref. 10.
e) Ref. 21. Polarizabilities of Mn^{2+}, Co^{2+}, and Ni^{2+} are assumed to be the same as that of Zn^{2+}.

dimensionally-linked interstitial spaces.[19]

The $M^{II}Zr_4(PO_4)_6$ compound with the β-$Fe_2(SO_4)_3$-type structure showed an order-disorder transition in the middle-temperature region. This phase transition may facilitate a widening of the bottle-neck of the ionic conduction pathway, in contrast to the situation in NASICON-type compounds. Further, the phase-transition temperature becomes higher upon decreasing the ionic size, due to the increased interaction between the guest cation and the framework.

(iii) Optimum Combination: Although the conduction behavior of $M^{II}ZP$ with the β-$Fe_2(SO_4)_3$-type structure may be somewhat different from that with the NASICON-type, there exists a common feature: There is a best combination between the size of guest cation and that of host framework, MnZP for the NASICON-type framework and ZnZP for the β-$Fe_2(SO_4)_3$-type.

(iv) Predominant Factor for the Ionic Conduction: In order to deduce the predominant factor regarding ionic conduction in NASICON- and β-$Fe_2(SO_4)_3$-type frameworks, the ionic conductivity of $M^{II}ZP$ at 900 °C was plotted as functions of the ionic radius[10] and the polarizability[22] of the mobile cation (cf. Fig. 5). The number in parentheses represents the value of log (σT) corrected for the porosity and electronic transport number. Figure 5 indicates that the conductivity of $M^{II}ZP$ with the NASICON-type structure (M^{II}=Mn, Cd, Ca, Sr, Pb, and Ba) changes drastically with the ionic radius of the mobile cation, that the cationic size does not affect the conductivity of the $M^{II}ZP$ with the β-$Fe_2(SO_4)_3$-type structure (M^{II}=Ni, Mg, Zn, Co, and Mn), as is found in a NASICON-type compounds, and that the cation which has a higher polarizability also shows a higher conductivity for the different two cations having almost the same cationic size for some compounds of the NASICON- (cf. BaZP and SrZP) and β-$Fe_2(SO_4)_3$-type (cf. MnZP and MgZP) structures. Hence, it is concluded that the predominant factor regarding ionic conduction in the zirconium phosphate framework is the ionic size of the mobile cation.

The authors would like to thank Dr. Tetsuo Uchida for the ICP emission spectroscopy, and Dr. Hitoshi Ohsato for his help in computing the lattice parameters. This work was partially supported by a research grant from the Toyoda Physical and Chemical Research Institute.

References

1) H. Y. -P. Hong, *Mater. Res. Bull.*, **11**, 173 (1976).
2) J. B. Goodenough, H. Y. -P. Hong, and J. A. Kafaras, *Mater. Res. Bull.*, **11**, 203 (1976).
3) S. Ikeda, M. Takahashi, J. Ishikawa, and K. Ito, *Solid State Ionics*, **23**, 125 (1987).

4) S. Ikeda, Y. Kanbayashi, K. Nomura, A. Kasai, and K. Ito, *Solid State Ionics,* **40/41**, 79 (1990).
5) K. Nomura, S. Ikeda, K. Ito, and H. Einaga, *J. Electroanal. Chem. Interfacial Electrochem.,* **326**, 351 (1992).
6) P. C. Christidis and P. J. Rentzeperis, *Z. Kristallogr.,* **141**, 233 (1975).
7) M. Menetriere, A. Levasseur, and P. Hagenmuller, *J. Electrochem. Soc.,* **131**, 1971 (1984).
8) I. Yokota, *J. Phys. Soc. Jpn.,* **16**, 2213 (1961).
9) R. D. Shannon, *Acta Crystallogr., Sect. A,* **32**, 751 (1976).
10) F. Sudreau, D. Petit, and J. P. Boilot, *J. Solid State Chem.,* **83**, 78 (1989).
11) S. Chandra, "Super Ionic Solids," Elsevier, North-Holland, New York (1981), Chap. 5.
12) J. Alamo and R. Roy, *J. Mater. Sci.,* **21**, 444 (1986).
13) L. Hagman and P. Kierkegaard, *Acta Chem. Scand.,* **22**, 1822 (1968).
14) M. Sljukic, B. Matkovic, B. Prodic, and D. Anderson, *Z. Kristallogr.,* **130**, 148 (1969).
15) G. E. Lenain, H. A. Mckinstry, J. Alamo, and D. K. Agrawal, *J. Mater. Sci.,* **22**, 17 (1987).
16) to be published.
17) H. Kohler and H. Schulz, *Mater. Res. Bull.,* **20**, 1461 (1985).
18) H. Kohler and H. Schulz, *Mater. Res. Bull.,* **21**, 23 (1986).
19) F. d'Yvoire, M. P-Screpel, E. Bretey, and M. Rochere, *Solid State Ionics,* **9/10**, 851 (1983).
20) I. P. Kondratyuk, B. A. Maksimov, and L. A. Muradyan, *Sov. Phys. Dokl.,* **32**, 95 (1987).
21) B. A. Maksimov, L. A. Muradyan, E. A. Genkina, and I. A. Verin, *Sov. Phys. Dokl.,* **31**, 348 (1986).
22) R. Kiriyama and H. Kiriyama, "Kozo Mukikagaku (Structural Inorganic Chemistry)," 3rd ed, Kyoritsu Shuppan, Tokyo (1979), Vol. 1, p. 242.